Received: 20 April 2023 | Revised: 18 July 2023 | Accepted: 8 August 2023

DOI: 10.1111/gcb.16926

Global Change Biology WILEY

RESEARCH ARTICLE

Ecosystem feedbacks constrain the effect of day-to-day weather variability on land–atmosphere carbon exchange

Edward B. Rastetter[1] | Kevin L. Griffin[2,3,4] | Bonnie L. Kwiatkowski[1] | George W. Kling[5]

[1]The Ecosystems Center, Marine Biological Lab, Woods Hole, Massachusetts, USA

[2]Department of Earth and Environmental Sciences, Columbia University, Palisades, New York, USA

[3]Department of Ecology, Evolution and Environmental Biology, Columbia University, New York, New York, USA

[4]Division of Biology and Paleo Environment, Lamont-Doherty Earth Observatory, Columbia University, Palisades, New York, USA

[5]Department of Ecology and Evolutionary Biology, University of Michigan, Ann Arbor, Michigan, USA

Correspondence
Edward B. Rastetter, The Ecosystems Center, Marine Biological Lab, Woods Hole, MA 02540, USA.
Email: erastetter@mbl.edu

Funding information
Division of Environmental Biology, Grant/Award Number: 1637459, 2220863, 1753731, 1651722, 1556772 and 2224743; Division of Polar Programs, Grant/Award Number: 1936769; National Science Foundation

Abstract

Whole-ecosystem interactions and feedbacks constrain ecosystem responses to environmental change. The effects of these constraints on responses to climate trends and extreme weather events have been well studied. Here we examine how these constraints respond to changes in day-to-day weather variability without changing the long-term mean weather. Although environmental variability is recognized as a critical factor affecting ecological function, the effects of climate change on day-to-day weather variability and the resultant impacts on ecosystem function are still poorly understood. Changes in weather variability can alter the mean rates of individual ecological processes because many processes respond non-linearly to environmental drivers. We assessed how these individual-process responses to changes in day-to-day weather variability interact with one another at an ecosystem level. We examine responses of arctic tundra to changes in weather variability using stochastic simulations of daily temperature, precipitation, and light to drive a biogeochemical model. Changes in weather variability altered ecosystem carbon, nitrogen, and phosphorus stocks and cycling rates in our model. However, responses of some processes (e.g., respiration) were inconsistent with expectations because ecosystem feedbacks can moderate, or even reverse, direct process responses to weather variability. More weather variability led to greater carbon losses from land to atmosphere; less variability led to higher carbon sequestration on land. The magnitude of modeled ecosystem response to weather variability was comparable to that predicted for the effects of climate mean trends by the end of the century.

KEYWORDS
carbon balance, climate change, C–N–P interactions, ecosystem biogeochemistry, ecosystem feedbacks, Jensen's inequality, weather variability

1 | INTRODUCTION

The constraints imposed by within-ecosystem interactions and feedbacks on responses to climate change are widely recognized. Most assessments address ecosystem responses to trends in carbon dioxide (CO_2) and climate (e.g., Arora et al., 2020; Campbell et al., 2009; Eby et al., 2013; Iverson et al., 2017; Luo et al., 2008; McGuire et al., 2018; Monier et al., 2017, 2018; Rastetter, Kwiatkowski, et al., 2022; Rollinson et al., 2017; Valipour et al., 2021; Wang et al., 2019; Wu et al., 2019). Studies that address climate variability usually focus on extreme events (Cleverly et al., 2019; De Boeck et al., 2018; Hughes et al., 2019; Knapp et al., 2008; Rammig & Mahecha, 2015). Variability of the environment, independent of extreme events, can also affect ecosystem function (Bernhardt et al., 2020; Medvigy et al., 2010; Paschalis et al., 2015; Rudgers et al., 2018; Ruel & Ayres, 1999; Seddon et al., 2016).

Several studies have examined the effects of interannual variability or regional patterns in precipitation on grassland production (e.g., Lauenroth & Sala, 1992; Sala et al., 1988). At a physiological and even daily time scale, photosynthesis increases asymptotically with the *amount* of soil water (because of the non-linear relation of soil water volume to soil water potential, e.g., Keenan et al., 2010; Kim & Verma, 1991), but annual production in these studies increased linearly with the *supply rate* of the major limiting resource, precipitation. This discrepancy in the curve shape of daily versus annual responses is likely due to both the metric used to quantify water availability (amount vs. supply rate) and to the time required for whole-plant response to changes in resource limitation. The slope of the within-site response to interannual variability in precipitation is much shallower (weaker) than the slope of among-site response to regional differences in the mean precipitation (Lauenroth & Sala, 1992), suggesting greater long-term adaptation of the community structure (species present), productivity, and ecosystem biogeochemistry at the regional scale.

Beyond these studies of interannual variability only a few studies have analyzed how changes in day-to-day weather variability might impact ecosystem function (e.g., Knapp et al., 2002, 2008; Paschalis et al., 2015). Changes in day-to-day weather variability should alter the mean rates of individual ecosystem processes because many of these processes respond non-linearly to environmental drivers (Supporting Information Jensen's inequality, Figure S1; Jensen, 1906; Knapp et al., 2008; Rastetter et al., 1992; Ruel & Ayres, 1999; Seddon et al., 2016; Templeton & Lawlor, 1981). Because of this non-linearity, the mean process rate will shift toward the concave side of the response curve if variability increases. For example, by artificially altering intervals between precipitation events without altering total annual precipitation, Knapp et al. (2002) found that grassland production decreased with increased variability in soil water content. This result is consistent with expectation of Jensen's inequality if the production response to soil water is concave downward (e.g., conceptual response in Knapp et al., 2008, Figure 1). Both Gherardi and Sala (2019) and Rudgers et al. (2018) report similar results, but it is difficult to separate effects of changes in variability from changes in the mean because their analyses are based on the coefficient of variation (variance/mean).

Two questions must be answered before the effects of day-to-day weather variability on ecosystem function can be assessed: (1) How will climate change affect day-to-day weather variability? and (2) what are the net-ecosystem effects of the individual-process responses to changes in weather variability in the context of whole-ecosystem interactions and feedbacks? We cannot answer the first question because there is currently a debate on whether subseasonal weather variability is increasing (Alexander et al., 2006; Bathiany et al., 2018; Donat & Alexander, 2012) or decreasing (Blackport et al., 2021; Dai & Deng, 2021). Here we address the second question by using stochastic simulations of daily weather with control, less, or more variability in temperature, precipitation, and light to drive the multiple element limitation (MEL) model of terrestrial-ecosystem biogeochemistry (Rastetter, Kwiatkowski, et al., 2022). We assess the effects of changes in day-to-day weather variability on carbon (C), nitrogen (N), phosphorus (P), and water stocks and cycling rates in arctic tundra as an example. We then compare those effects to modeled responses of tundra to long-term climate trends of increasing CO_2, temperature, and precipitation. We conclude that changes in weather variability can have impacts on terrestrial C storage or C loss to the atmosphere that are comparable in magnitude to the impacts of the long-term climate trends, and thus could affect regional to global warming.

2 | METHODS

2.1 | Model

For our analysis, we used the MEL model, a process-based model of the interactions among C, N, P, and water cycles in terrestrial ecosystems (Rastetter et al., 1997, 2013; Rastetter, Kwiatkowski, et al., 2022; Rastetter & Shaver, 1992). The model has been calibrated and applied to many terrestrial ecosystems (e.g., Rastetter, Kwiatkowski, et al., 2022) including tussock tundra near Toolik Lake, AK (Jiang et al., 2015; Pearce et al., 2015), with a full description of the model and its calibration in Rastetter, Kwiatkowski, et al. (2022). A key characteristic of this model is an acclimation algorithm that reallocates resource acquisition effort of plants from less-limiting resources to more-limiting resources. For example, during drought periods, the algorithm will reallocate effort from light capture and carboxylation and redirect it toward water uptake (Rastetter & Kwiatkowski, 2020). Similarly, resource acquisition effort is redistributed among C, N, and P to maintain plant stoichiometry. Equations in the model also assure the analogous stoichiometric balance in resource acquisition by soil microbes. These acclimation algorithms mean that if the availability or acquisition rate of one resource is changed by a change in the variability of one of the drivers (e.g., light or temperature), the model will respond by reestablishing the stoichiometric balance of the system. The model has several processes that are driven directly

by air temperature and light, or indirectly from temperature, precipitation, and light through a soil energy budget to calculate soil temperature or through a soil water budget to calculate soil water volume and soil water potential (Figure 1; Table 1).

2.2 | Stochastic weather generator

To change variability in weather, we developed a stochastic weather generator for daily precipitation, light, and maximum and minimum daily temperature (described in Supporting Information; Table S1; Figures S2–S4). The weather generator reproduces the seasonal distributions and statistical properties of the 1989–2019 climate record of the NSF Arctic Long-Term Ecological Research (ARC-LTER) site near Toolik Lake, AK (Environmental Data Center Team, 2021; Rastetter, Griffin, et al., 2022a).

We generated 10 replicate sets of nine, 100-year weather records (described below). All nine weather records within a set were generated with the same time series of random numbers and therefore had the same underlying stochastic drivers and are correlated. The nine records within a set differed only in the values of the parameters that determine variability in precipitation, light, and temperature (Table S1: α_P in Equation S3, α_D in Equation S4, β_λ in Equation S10, and γ_T in Equation S14). Among the 10 replicate sets of weather records, the random numbers, and therefore the weather records, are independent of one another. To adjust all 90 weather records to the same 100-year mean precipitation, light, and temperature, we calculated correction factors for each weather record (Table S1: Ψ_R in Equation S6 for precipitation; Ψ_λ in Equation S12 for light; and Ψ_T in Equation S15 for maximum and minimum temperature).

We generated three primary records for each of the 10 replicate sets of weather records:

1. The control record had properties similar to the measured Toolik Lake data (Table S1; Figures S2–S4). The standard deviation in average daily temperature was ~10°C in the winter and ~4°C in the summer; the average duration of periods of precipitation was ~2.7 days; the average duration of dry periods was ~5.1 days; ~48% of days had more than 90% of maximum possible light for that day of the year ($\lambda > 0.9\ \lambda_{max}$); and ~6% of days had less than 40% of maximum light for that day of the year ($\lambda < 0.4\ \lambda_{max}$).

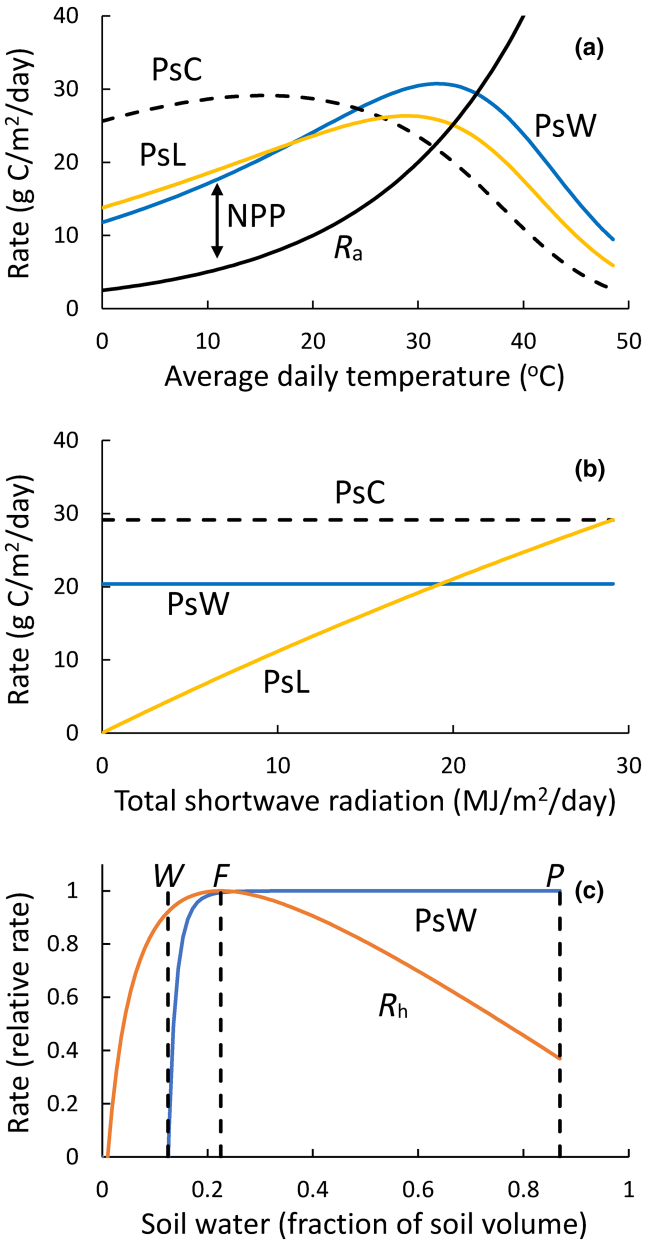

FIGURE 1 Instantaneous responses of some major processes in the biogeochemical model to changes in temperature, precipitation, and light. (a) Responses of autotrophic respiration (R_a) and photosynthesis that is CO_2 limited (PsC), light limited (PsL), and water limited (PsW) to changes in temperature. Net primary production (NPP) is the difference between the most limiting photosynthesis rate and R_a. On a seasonal timescale, the three photosynthesis curves will change vertically relative to one another depending on the effort allocated to them in the optimization routine of the model and the leaf area. The light-limited curve will change with daily changes in total shortwave radiation. The water-limited curve will change with available soil water, including the decrease in available water in proportion to the fraction of soil that is frozen. The autotrophic respiration curve has the same shape as that for nutrient uptake and microbial metabolism, including heterotrophic respiration (R_h), and soil nutrient cycling. (b) Response of photosynthesis to changes in total shortwave radiation. Light-limited photosynthesis is only slightly concave downward because of the scaling to a daily time step. However, at high light the overall photosynthetic rate will be either CO_2 limited or water limited, giving a concave-downward, asymptotic overall response. Again, the three curves will change relative to one another as allocation of effort and environmental conditions change. (c) Responses of water-limited photosynthesis and microbial metabolism (represented by heterotrophic respiration) to changes in soil water. Decline in microbial metabolism with waterlogging is due to inhibition of O_2 diffusion. Dashed lines indicate wilting point (*W*), field capacity (*F*), and porosity (*P*) for this peat soil. Equations, assumption, parameters, and sources are in Rastetter, Kwiatkowski, et al. (2022).

TABLE 1 Instantaneous responses of some major processes in the biogeochemical model to changes in temperature, precipitation, and light.

Process	Temperature	Precipitation	Light
GPP	Unimodal concave up at low temperature (+), down near optimum temperature (−)	Asymptotic concave down through soil moisture (−)	Asymptotic concave down (−)
R_a	Exponential concave-up Q_{10} function through air and soil (roots) temperature (+)	None	Exponential concave-up Q_{10} function of roots respiration through soil heat budget (+)
NPP = GPP − R_a	Unimodal concave down (−); stronger concavity of R_a than GPP	Asymptotic concave down through soil moisture (−)	Asymptotic concave down (−); stronger concavity of GPP than R_a
R_h	Exponential concave-up Q_{10} function through soil temperature (+)	Unimodal concave down on soil moisture (includes effect of low O_2 with waterlogging) (−)	Exponential concave-up Q_{10} function through soil heat budget (+)
N uptake	Exponential concave-up Q_{10} function through soil temperature (+)	Linear with soil water	Exponential concave-up Q_{10} function through soil heat budget (+)
N immobilization	Exponential concave-up Q_{10} function through soil temperature (+)	Unimodal concave down on soil moisture (includes effect of low O_2 with waterlogging) (−)	Exponential concave-up Q_{10} function through soil heat budget (+)
Gross N mineralization	Exponential concave-up Q_{10} function through soil temperature (+)	Unimodal concave down on soil moisture (includes effect of low O_2 with waterlogging) (−)	Exponential concave-up Q_{10} function through soil heat budget (+)
Net N mineralization	Exponential concave-up Q_{10} function through soil temperature (+)	Unimodal concave down on soil moisture (includes effect of low O_2 with waterlogging) (−)	Exponential concave-up Q_{10} function through soil heat budget (+)
P uptake	Exponential concave-up Q_{10} function through soil temperature (+)	Linear with soil water	Exponential concave-up Q_{10} function through soil heat budget (+)
P immobilization	Exponential concave-up Q_{10} function through soil temperature (+)	Unimodal concave down on soil moisture (includes effect of low O_2 with waterlogging) (−)	Exponential concave-up Q_{10} function through soil heat budget (+)
Gross P mineralization	Exponential concave-up Q_{10} function through soil temperature (+)	Unimodal concave down on soil moisture (includes effect of low O_2 with waterlogging) (−)	Exponential concave-up Q_{10} function through soil heat budget (+)
Net P mineralization	Exponential concave-up Q_{10} function through soil temperature (+)	Unimodal concave down on soil moisture (includes effect of low O_2 with waterlogging) (−)	Exponential concave-up Q_{10} function through soil heat budget (+)

Note: (+) indicates that the average process rate is positively correlated with the magnitude of variance in the variable in the column heading. (−) indicates that the average process rate is negatively correlated with the magnitude of variance in the variable in the column heading. Equations, assumption, parameters, and sources are in Rastetter, Kwiatkowski, et al. (2022).

Abbreviations: GPP, gross primary production; NPP, net primary production; R_a, autotrophic respiration; R_h, heterotrophic respiration; VPD, vapor pressure deficit.

2. For the record with less variability, we used the same series of random numbers as used for the control. The variance in daily average temperature was reduced (Table S1, γ_T decreased) so that the standard deviation of temperature decreased by ~3°C relative to the control for the entire year. The duration of periods of precipitation was about 1 day longer than the control (α_P larger) and the duration of the dry periods was about 1 day shorter (α_D smaller), thereby forcing the same total rainfall for the 100-year record into more days, spreading precipitation more evenly over time, and less day-to-day rainfall variability. We lowered its light variance (β_λ smaller) so that 44% of days had more than 90% of maximum light for that day of the year ($\lambda > 0.9\ \lambda_{max}$) and 0.4% of days had less than 40% of maximum light ($\lambda < 0.4\ \lambda_{max}$).
3. For the record with more variability, we again used the same series of random numbers as used for the control. The variance in daily average temperature was increased (Table S1, γ_T increased) so that the standard deviation of temperature increased by ~3°C over the control for the entire year. The duration of periods of precipitation was about 1 day shorter than the control (α_P smaller) and the duration of the dry periods about 1 day longer (α_D larger), thereby forcing the same total rainfall for the 100-year record into fewer days and more day-to-day rainfall variability. The variance in light was increased (β_λ larger) so that 51% of days had more than 90% of maximum light for that day of the year ($\lambda > 0.9\ \lambda_{max}$) and 11% of days had less than 40% of maximum light ($\lambda < 0.4\ \lambda_{max}$).

To assess the individual effects of each weather variable, we assembled an additional six weather records from components of these three primary weather records (nine weather records total in each of the 10 sets). These additional weather records had the following properties:

4. A record with less variability in temperature only, using the temperature record from the less variability record 2 above, but precipitation and light from the control record 1 above.
5. A record with more variability in temperature only, using the temperature record from the more variability record 3 above, but precipitation and light from the control record 1 above.
6. A record with less variability in precipitation only, using the precipitation record from the less variability record 2 above, but light and temperature from the control record 1 above.
7. A record with more variability in precipitation only, using the precipitation record from the more variability record 3 above, but light and temperature from the control record 1 above.
8. A record with less variability in light only, using the light record from the less variability record 2 above, but precipitation and temperature from the control record 1 above.
9. A record with more variability in light only, using the light record from the more variability record 3 above, but precipitation and temperature from the control record 1 above.

Because of the way we assembled these weather records, all records share identical time series for the individual weather components with the other records in the same set and are in this sense partly synchronized. We imposed this synchronization among weather records within a set to facilitate analysis of the contribution of each of the individual weather components on ecosystem response to changes in variability in all the weather components combined. By assessing responses to less or more variability relative to the control within the same set of simulations (i.e., paired comparisons), the synchronization also helped isolate the effects of variance from the idiosyncratic effects of the specific random-number series.

2.3 | Simulations

We ran 90 simulations with the MEL model driven with data from the stochastic weather records described above and with no climate trend. All the simulations used the same parameter values from the calibration for tussock tundra (Rastetter, Kwiatkowski, et al., 2022). For each of the 10 sets of weather records, we generated initial conditions by running a 1000-year simulation using the control weather record for that set (10 times through record 1 above) and saving the final modeled conditions to initialize all nine simulations within that set. Thus, within a set, all simulations began from the same initial conditions. The only difference among simulations within a set was in the weather record used to drive the model. Even with this model initialization, the ecosystem accumulated about 0.27 g C m^{-2} over 100 years in the control simulation (i.e., very close to but not at steady state; Table 2). Parameter

TABLE 2 Changes in vegetation, soil, and total-ecosystem carbon (C) for 10 replicate model runs averaged over the last 10 years of a 100-year simulation with less, control, and more weather variability.

		No climate trend			With climate trend		
		Less variability	Control	More variability	Less variability	Control	More variability
Mean change (g C m^{-2})	Veg C	122.9	14.2	−176.8	491.6	440.0	357.4
	Soil C	95.6	13.1	−358.9	−134.1	−167.1	−290.6
	Total C	218.5	27.3	−535.8	357.5	272.9	66.9
Std error (g C m^{-2})	Veg C	23.7	27.0	20.1	17.4	17.5	18.9
	Soil C	42.2	48.6	49.8	41.2	41.7	43.6
	Total C	45.8	42.9	49.8	45.5	42.6	43.0
Max (g C m^{-2})	Veg C	240.6	123.9	−80.8	569.4	525.8	445.3
	Soil C	159.9	64.2	−181.9	−90.0	−129.3	−270.6
	Total C	296.7	121.0	−335.1	444.9	338.5	154.3
Min (g C m^{-2})	Veg C	−47.9	−157.6	−276.1	376.3	334.3	242.9
	Soil C	56.1	−75.3	−499.2	−171.5	−192.3	−324.2
	Total C	112.1	−93.3	−656.5	286.4	205.0	−43.6
Response effect (mean/$LSD_{0.05}$)	Veg C	2.0**	0.2	−2.8**	14.4**	12.9**	10.5**
	Soil C	0.6	0.1	−2.1**	−1.0*	−1.2*	−2.1**
	Total C	1.3*	0.2	−3.1**	2.3**	1.7**	0.4

Note: Responses to weather records with no climate trend (left columns) and with an imposed mean climate trend (right columns) are described in Section 2. The no climate trend weather records are the same as used for Figure 1. The response effect is the mean value divided by the $p < .05$ least significant difference ($LSD_{0.05}$); absolute magnitudes ≥1 indicate a significant change from the initial value at $^{*}p < .05$, absolute magnitudes ≥1.35 indicate a significant change at $^{**}p < .01$.

files, driver files, and results for these simulations are available from the Environmental Data Initiative (Rastetter, Griffin, et al., 2022b).

For our analyses of C, N, and P stocks, we used peak-season values (August 11). For our analyses of C, N, and P fluxes, we used annual cumulative rates. To remove the year-to-year variability from the long-term response, and to remove any bias from using a single year at the end of the record, we calculated mean values for all response variables over the last 10 years of the 100-year simulations. To assess significant changes from the control in the less- and more-variability simulations, we ran one factor (variability in either temperature or precipitation or light, or all three combined), three-level (less, control, and more variability) analysis of variance (ANOVA) on the 10 replicates of these 10-year means (Snedecor & Cochran, 1967; ANOVA tables assembled in Microsoft Office 365 Enterprise EXCEL). Based on these ANOVA, we calculated least significant differences (LSDs) at both the .05 and .01 probability levels (Snedecor & Cochran, 1967). To assess synergistic interactions among weather variables, we also calculated the sum of the responses to each of the three weather factors individually, along with the ANOVA and LSD analyses on the sum of the responses to individual weather factors.

Finally, to assess the importance of responses to changes in variability relative to responses to long-term climate trends, we ran an additional 30 simulations with less, control, or more variability in all three weather variables in combination with linear increases over 100 years in atmospheric CO_2, doubling from 400 to 800 μmol mol^{-1}, temperature by 3.5°C, and precipitation by 20% (this is the "climate mean trend"). Parameter files, driver files, and results for these simulations are available from the Environmental Data Initiative (Rastetter, Griffin, et al., 2022c).

3 | RESULTS

Changing the day-to-day variability of all three weather variables together had significant effects on C storage in vegetation and soil within 5–15 years from the start of the 100-year simulation (Figure 2). Averaging the last 10 years of the simulation, with less variability the vegetation C increased 109 g C m^{-2} above the control ($p < .01$) and with more variability it decreased 191 g C m^{-2} below the control ($p < .01$) (Figures 1a and 2a,b; Table 2). These areal changes in C are 1.7 and 3.1 times greater than the $p = .05$ LSDs (Table 2). The 82.5 g C m^{-2} increase in soil C above control with less variability in the weather variables in combination was not significant, but with more variability soil C decreased by 372 g C m^{-2} below the control ($p < .01$) (Figures 1b and 2a,b; Table 2). The gain in vegetation C with less variability was enough to increase the total-ecosystem C 191 g C m^{-2} above the control ($p < .05$), even without a significant increase in soil C (Figures 1c and 2a,b; Table 2). With more variability, the significant C losses from both vegetation and soil led to a total-ecosystem loss of 563 g C m^{-2} below the control ($p < .01$) (>99% lost as CO_2). The magnitudes of these losses are comparable to the gains predicted under the mean climate change trend using this same model (Rastetter, Kwiatkowski, et al., 2022).

Changes in C stocks result directly from changes in ecosystem fluxes of C, and indirectly from fluxes of N and P. These fluxes

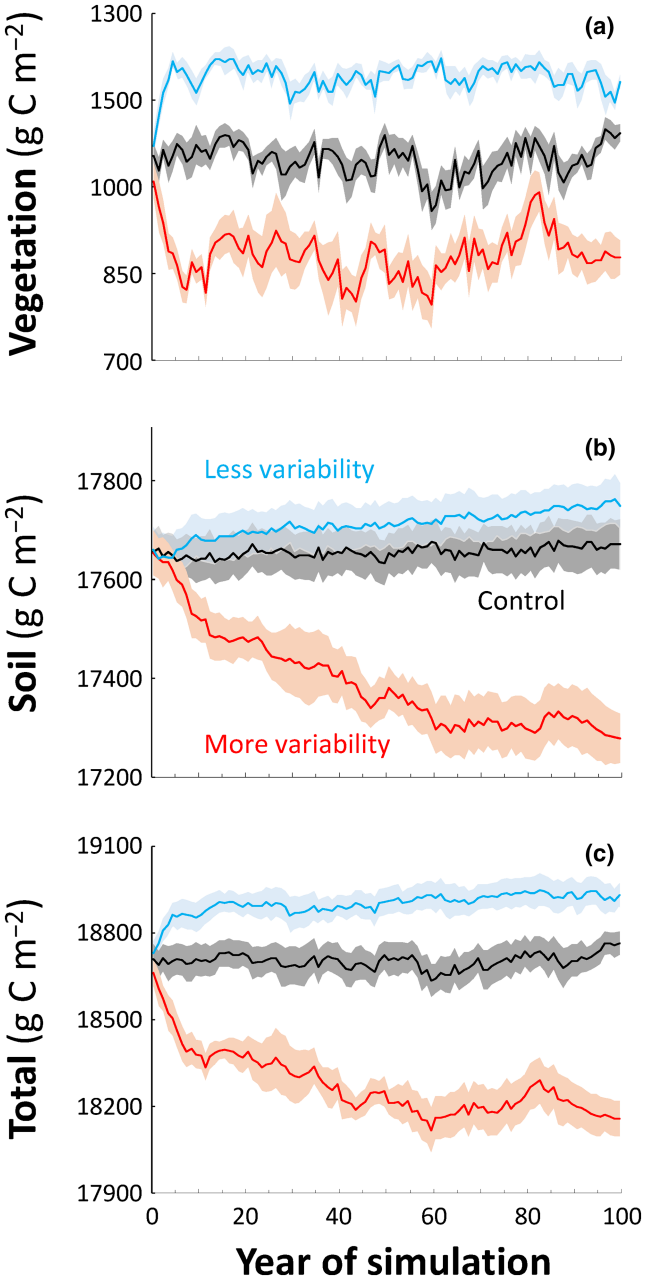

FIGURE 2 Simulated changes in tussock tundra (a) vegetation, (b) soil, and (c) ecosystem carbon to the baseline control (black), less (blue), and more (red) variability of precipitation, light, and temperature using synthetic weather records (Table S1). The simulations use the multiple element limitation model and a single parameter set. Graphs show the mean responses (solid line) and standard error of the mean (shaded region) of 10 replicate weather records for control (same variability as the Toolik Field Station record), less (same precipitation over 38% more days, 9% fewer bright and 93% fewer dim days, and 3°C decreased temperature standard deviation, SD), and more (same precipitation in 36% fewer days, 4.5% more bright, and 76% more dim days, and 3°C increased temperature SD) variability simulations. All weather records were adjusted to the same mean precipitation, temperature, and irradiance; only the day-to-day variability changed. Simulations are first initialized by running the model for 1000 years under the control weather (10 times though the control synthetic weather record).

include gross primary production (GPP), autotrophic and heterotrophic respiration (R_a and R_h), uptake of N and P by plants, litterfall amounts of C, N, and P, and net N and P mineralization in the soil (Figure 4). Changes in the daily variability of average temperature had stronger effects on these fluxes than did changes in variability of precipitation or light (Figure 4). GPP is a unimodal function of temperature that is concave up at lower temperature and concave down as temperature approaches the optimum. Even at lower temperature, the concave-up curvature of GPP is weaker than the concave-up curvature of R_a. Thus, the effect of less temperature variability is to increase net primary production (NPP = GPP − R_a) and the effect of more temperature variability is to decrease NPP. The significant increase in GPP with less temperature variability ($p < .01$, Figure 4) is mostly the effect of increased biomass with increased NPP rather than a direct effect of Jensen's inequality on GPP. Similarly, the significant decrease in GPP with more temperature variability ($p < .05$; Figure 4) is mostly the effect of decreased biomass with decreased NPP rather than a direct effect of Jensen's inequality. With concave-up responses to temperature, the fluxes R_a, R_h, N, and P uptake by plants, and net N and P mineralization, are all expected to decrease with less temperature variability and increase with more temperature variability; however, all fluxes did the opposite in the long term (all significant at $p < .01$ except for N uptake by plants where $p < .05$ for both less and more variability and R_a with more variability is not significant; Figure 4). The decrease in R_a with more variability was not significant because an increase in biomass overrides the direct effects of Jensen's inequality in the long term. In the model, changes in temperature variability have no direct effect on litterfall, but, because of the change in biomass, litterfall C, N, and P all increased significantly with less variability and decreased significantly with more variability ($p < .01$). In the long term, the net result was a significant ($p < .01$) increase in vegetation C, N, and P with less temperature variability and a significant ($p < .01$) decrease in vegetation C, N, and P with more temperature variability (Figure 3), which in turn feeds back to alter the rates of plant-mediated processes, as just described. There were no significant changes in soil or total-ecosystem C, N, or P with less temperature variability. With more temperature variability there was a significant ($p < .01$) loss of soil and total-ecosystem C, but no significant change in soil or total-ecosystem N or P (Figure 3).

The responses to changes in precipitation variability were weaker than responses to changes in temperature variability. The only significant response to a change in precipitation variability was an increase in litterfall P with less variability ($p < .05$, Figure 4), even though there is no direct effect of moisture on litterfall in the biogeochemical model. This increase in litterfall P resulted from a significant increase in vegetation P with less variability ($p < .05$) despite no significant increase in the plant uptake rate of P (Figure 3). There were no significant changes in either metabolic rates or stocks of C, N, or P with more variability in precipitation (Figures 3 and 4).

Responses to changes in variability of light (cloudiness) were also weak (Figures 2 and 3). Jensen's inequality for the asymptotic, concave-down relation of GPP to light predicts that less light variability will increase GPP, and more light variability will decrease GPP; both expectations were met, but neither was significant (Figure 4). There is no direct effect of changes in light variability on aboveground autotrophic respiration or litterfall C, N, or P in the model. However, light is included in the soil energy budget (heat from incident radiation) and can thereby affect soil temperature and in turn microbially mediated processes. Through this indirect mechanism, belowground processes are expected to decrease with less light variability and increase with more light variability. Contrary to expectation, the only significant responses were increases in net P mineralization and plant uptake of P ($p < .05$) with less light variability (Figure 4), which was likely driven by the increase in GPP rather than the direct effects on the soil energy balance. This increase in P uptake resulted in a significant increase in vegetation P with less light variability (Figure 3).

When the changes in metabolic rates in response to variability of the three weather variables individually are added together, their sum is consistent in direction, magnitude, and significance level with the change in metabolic rates when the variability in all three weather variables is altered together (Figure 4). The exception is the increase in GPP with less variability, which is significant at $p < .01$ for the sum of individual effects of temperature, precipitation, and light alone and is only significant at $p < .05$ in all three variables together. N uptake with less weather variability did not change significantly, but all other responses are significant at $p < .01$. With less variability in the weather variables, these metabolic changes resulted in increased vegetation C, N, and P ($p < .01$) and increased total-ecosystem C ($p < .01$ for the sum of individual responses, $p < .05$ for all weather variables combined). With more variability in the weather variables, these metabolic changes resulted in decreased vegetation C, N, and P ($p < .01$), and decreased soil and total-ecosystem C ($p < .01$). Total-ecosystem P decreased significantly with all the weather variables combined ($p < .01$) but not with the sum of responses to the individual weather variables.

Imposing a gradual, linear climate trend over 100 years for atmospheric CO_2 (400–800 μmol mol^{-1}), mean temperature (+3.5°C), and precipitation (+20%) (see Section 2) changed the amount and distribution of C in the ecosystem but did not alter the relative ranking of responses to less, control, and more weather variability. That is, compared to the simulation with control variability, the C stored in vegetation, soil, or the whole ecosystem was always highest with less weather variability and lowest with more variability (Figure 5; Table 2). The model predicts gains in ecosystem C with the mean climate trend in all but two of the 10 replicate simulations, both of which had more weather variability. With the climate trend and control variability, the vegetation gained C (440 ± 18 g C m^{-2}) and the soil lost C (167 ± 42 g C m^{-2}), resulting in a net total-ecosystem gain of 273 ± 43 g C m^{-2} (± standard error of the mean) (Figure 5; Table 2). Less weather variability increased the net total-ecosystem gain to 358 ± 45 g C m^{-2}, but when the climate trend was coupled with more weather variability, this carbon gain was 80% lower and the total-ecosystem gain was only 67 ± 43 g C m^{-2}.

In our simulations, the C, N, and P cycles are tightly coupled. Across the nine core treatments in our study (control, low and high variability for temperature, precipitation, light, and all three combined), the values averaged over the last 10 years of the simulations and across

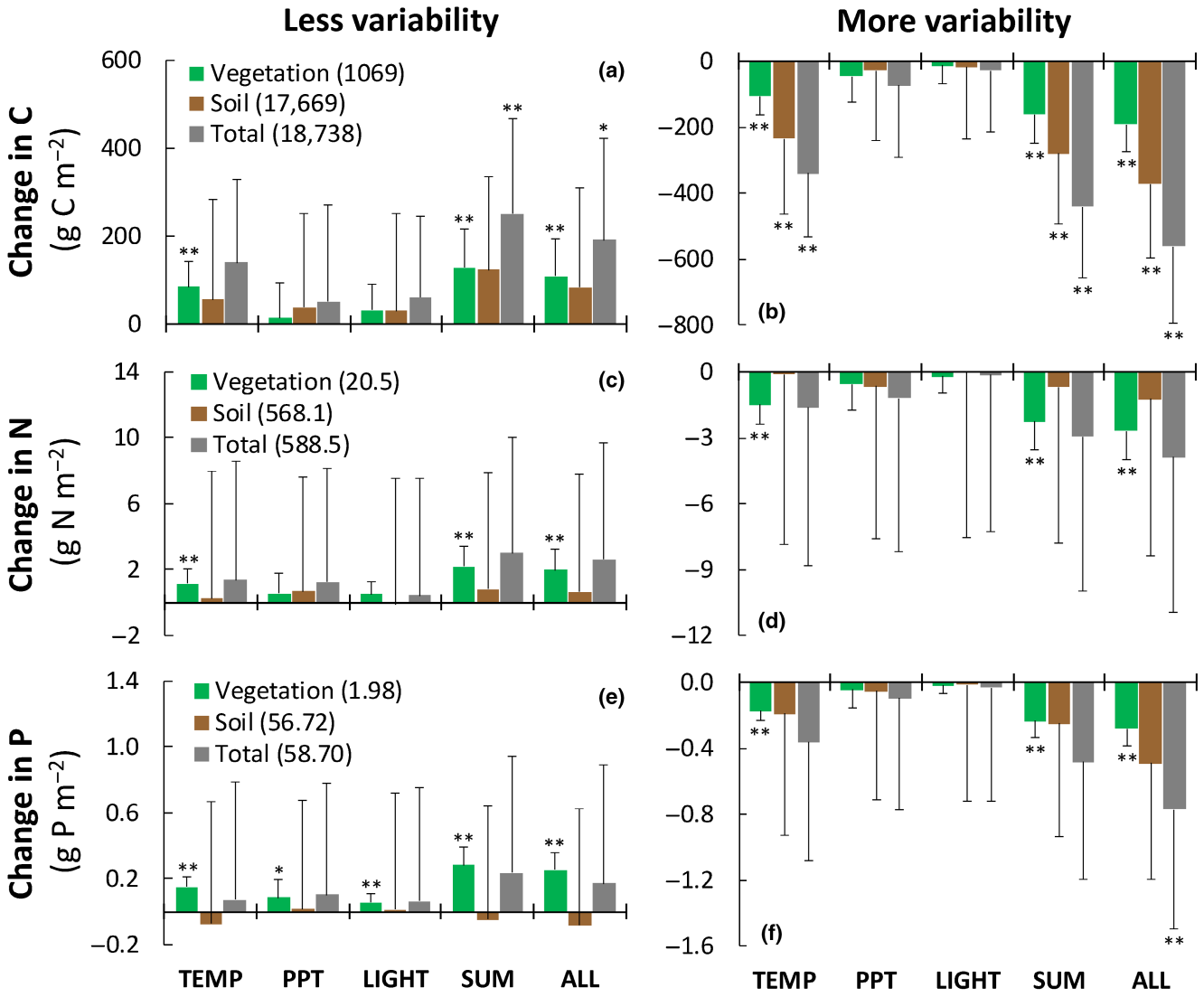

FIGURE 3 Average change from control for the last 10 years of the simulations for vegetation, soil, and total-ecosystem carbon (a, b), nitrogen (c, d), and phosphorus (e, f) with less (left) and more (right) variability in temperature (TEMP), precipitation (PPT), and total shortwave radiation (LIGHT) both individually and in combination (ALL) and for the sum of the effects of the three individual weather variables (SUM). The change is calculated relative to the control in the same set of nine simulations and the chart values are the average across the 10 sets of simulations (see Section 2). To help assess the magnitude of these changes, the numbers in parentheses in the legend are the average value of each variable in the last 10 years of all 10 control runs. Error bars are for $p < .01$ least significant differences (LSDs) based on an analysis of variance on the averages of the last 10 years of the 10 simulations for less-, control-, and more-variability simulations. "**" Indicates that the change is larger than the $p < .01$ LSD. "*" Indicates that the change is larger than the $p < .05$ LSD.

the 10 replicates for GPP, R_a, NPP, litterfall C, N, and P, uptake of N and P by plants, and net N and P mineralization, are all positively and strongly correlated (mean of the 45 Pearson's correlations $r = .95$, range .84–1.00, all $p < .01$). This tight coupling derives from the acclimation of both plants and microbes in the model to correct imbalances in stoichiometry, and as described below illustrates why Jensen's inequality used with single variables is inadequate to describe ecosystem responses.

4 | DISCUSSION

The mean temperature, precipitation, and light used to drive the model were constant in the core simulations (i.e., no imposed climate trend), and only the magnitude of day-to-day variability in one or in all three of the weather variables changed in our simulations. Thus, the only possible response in the model is through the direct effects of Jensen's inequality on individual processes and the subsequent cascade of interactions and feedbacks initiated by these direct effects. We found both statistically significant and ecologically meaningful responses to the changes in weather variability that were of magnitudes comparable to the modeled responses to future mean climate trends (Figure 5). The response to changes in temperature variability dominated the overall responses. However, of the processes we examined, only NPP responded to changes in variability as expected based on Jensen's inequality; the significant response of GPP was in the expected direction but was due to the

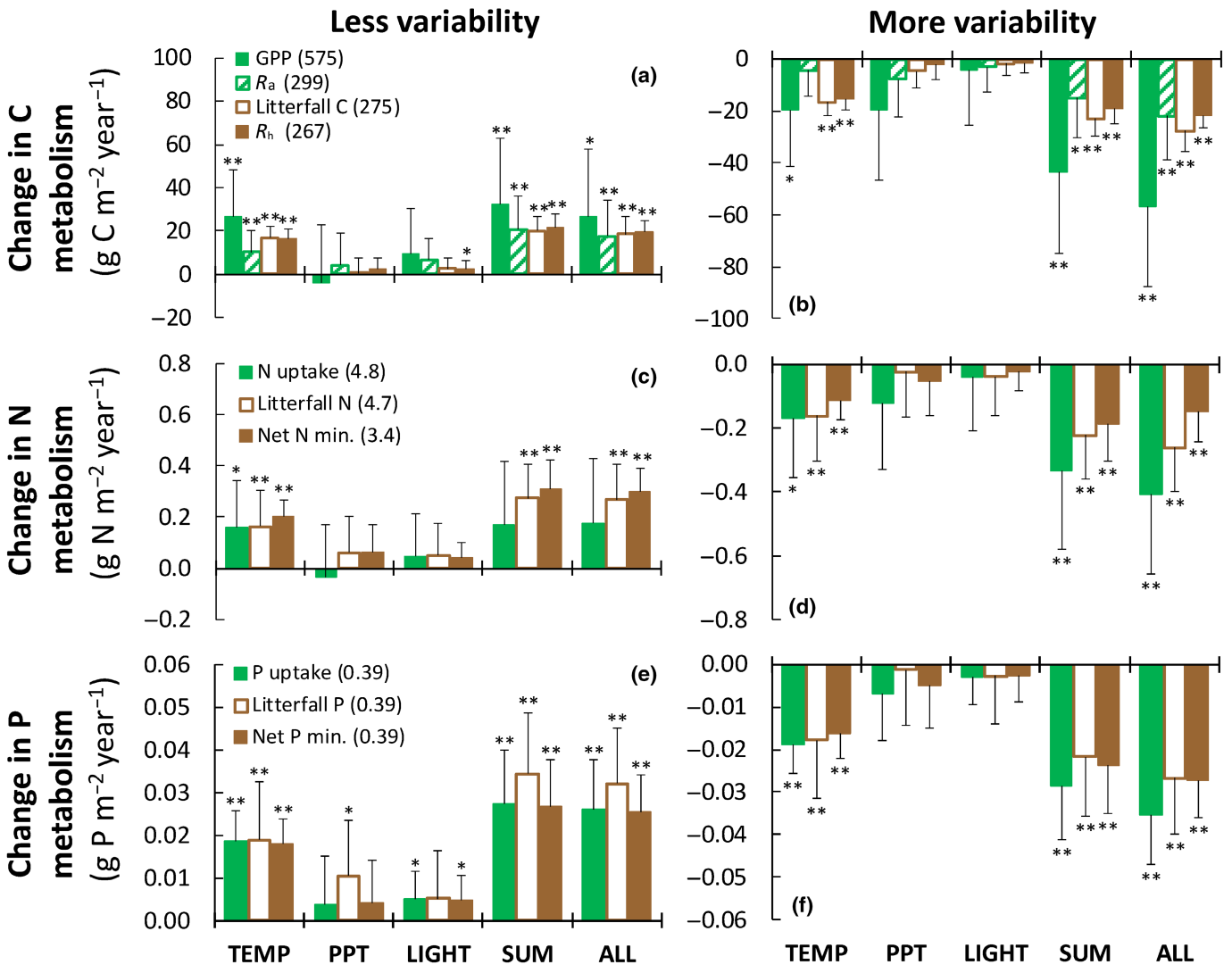

FIGURE 4 Average changes from control for the last 10 years of the 100-year simulations for the major components of the carbon (a, b), nitrogen (c, d), and phosphorus (e, f) metabolism with less and more variability in temperature (TEMP), precipitation (PPT), and total shortwave radiation (LIGHT) both individually and in combination (ALL) and for the sum of the effects of the three individual weather variables (SUM). The carbon metabolism is represented by gross primary production (GPP), autotrophic respiration (R_a), litterfall C, and heterotrophic respiration (R_h). The nitrogen metabolism is represented by total uptake of N by plants (NH_4, NO_3, and organic N), litterfall N, and net N mineralization. The phosphorus metabolism is represented by plant uptake of PO_4, litterfall P, and net P mineralization. The change is calculated relative to the control in the same set of nine simulations and the bars are the average change across the 10 sets of simulations (see Section 2). To help assess the magnitude of these changes, the numbers in the legend in parentheses are the average value of each variable in the last 10 years of all 10 control runs. Error bars are for $p < .01$ least significant differences (LSDs) based on an analysis of variance on the averages of the last 10 years of the 10 simulations for less-, control-, and more-variability simulations. "**" Indicates that the change is larger than the $p < .01$ LSD. "*" Indicates that the change is larger than the $p < .05$ LSD.

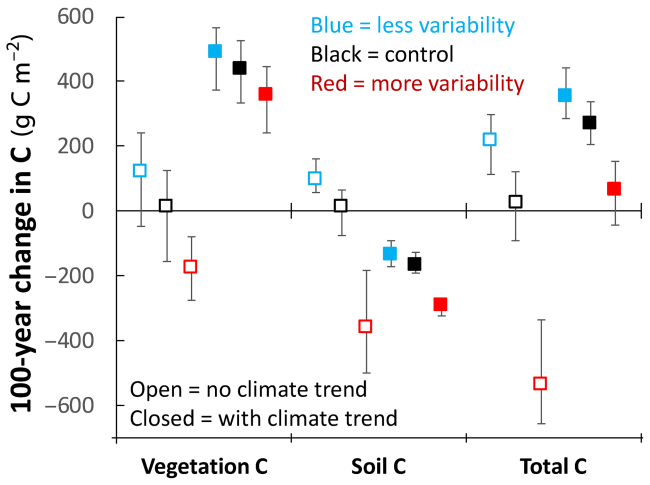

FIGURE 5 Mean changes in carbon over the 100-year simulations for vegetation, soil, and total ecosystem with less (blue), control (black), and more (red) variability in precipitation, light, and temperature, without (open symbols) and with (closed symbols) a climate trend (ramped doubling of CO_2, 3.5°C warming, and 20% increase in precipitation). Whiskers show the maximum and minimum values of 10 replicate simulations. All data are for changes in peak-season (August 11) values between year 1 of the control with no climate change simulation and the average over the last 10 years of the treatment simulations.

indirect effect of NPP on biomass rather than a direct effect of Jensen's inequality.

Our results indicate that Jensen's inequality applied to individual processes is an inadequate predictor of ecosystem response to changes in weather variability because of the interactions and tight coupling of element cycles in terrestrial ecosystems. This tight coupling is illustrated in our model results where ecosystem processes were highly correlated (mean Pearson's $r = .95$). In addition, in many mature terrestrial ecosystems, N and P cycle tightly (internal cycling >> supply from outside the ecosystem), and thus N and P cycles are coupled. Biomass production is tightly tied to these N and P cycling rates (Rastetter et al., 2013); NPP in Alaskan tussock tundra is known to be strongly nutrient limited (Shaver et al., 2014). If a change in weather variability results in the acceleration or deceleration of one element cycle relative to the others, then the cycles become decoupled. Any loss of coupling of the C, N, and P cycles resulting from the effects of a change in weather variability on individual processes must therefore be transient. That is, in the absence of continued major disturbances eventually the stoichiometric feedbacks in the ecosystem will act to recouple the cycles. For example, with less temperature variability the stronger concave-up relation of R_a than of GPP to temperature should result in an increase in NPP (see Section 3). However, the concave-up relation of net N and P mineralization to temperature should result in a decrease in nutrient supply with less temperature variability and should thereby limit NPP. Thus, the increase in NPP caused by less temperature variability on GPP and R_a cannot be maintained unless some mechanism increases the supply of N and P to vegetation and thereby overrides the Jensen's-induced nutrient limitation of NPP. Our simulations indicate that the acclimation of plant and microbe resource acquisition in our model results in such an override. Most importantly, the increase in NPP disrupts the vegetation stoichiometric balance so the MEL model reallocates resource acquisition effort from C to N and P. Vegetation is thereby able to compete more effectively with microbes for nutrients. Thus, less temperature variability caused net N and P mineralization to increase rather than decrease (Figure 4); this result illustrates that these secondary feedback effects can eventually overwhelm the initial effect of Jensen's inequality on individual processes. These secondary feedbacks are similar to the Lauenroth and Sala (1992) explanation for the weaker within-site sensitivity of production to interannual variability in precipitation relative to the stronger regional increase in production with increased precipitation among grassland sites. The pattern addressed by Lauenroth and Sala (1992) is driven by adaptation to persistent differences in *mean conditions* across the region (Estiarte et al., 2016). In contrast, our secondary feedback effects are driven by adaptation to persistent changes in day-to-day variability, which in turn alters the *mean response* because of the non-linearity.

In addition to ecosystem interactions and feedbacks modifying the direct response of a process to weather variability, some components of the ecosystem are likely buffered from day-to-day variability. For example, aboveground plant components respond directly to changes in air temperature. However, root and soil components respond to changes in air temperature indirectly through a soil energy budget, which is buffered by the soil thermal mass, resulting in lower variability in soil temperature and thus a weakened effect of Jensen's inequality. Similarly, responses to variability in precipitation are buffered by the soil water budget. Responses to changes in precipitation should increase as water becomes more limiting (Huxman et al., 2004), thus, more mesic soils should be more sensitive to changes in day-to-day variation of precipitation, as found by Knapp et al. (2002). The temporal scale of the variability relative to the response time of the ecosystem components likely also plays a role in the overall response. Thus, stronger responses have been found for changes in year-to-year variation in precipitation where the vegetation has more time to respond (Baldocchi et al., 2018; Gherardi & Sala, 2019; Hou et al., 2021; Knapp & Smith, 2001; Sala et al., 1988).

The dominant ecosystem response to weather variability was to increase element cycling rates and storage when variability was lowered, and to decrease cycling rates and storage when variability was raised (Figures 2–5; Table 2). Similar trends have been found for changes in the frequency of disturbances that remove element stocks (Luo & Weng, 2011; Valipour et al., 2021), but for different reasons because no element stocks are directly removed in our simulations. This superficial similarity arises because the decrease in NPP with increased variability decreases the ability of the ecosystem to retain elements, rather than the direct removal of elements by disturbance.

The responses of ecosystem C storage and loss to the atmosphere as greenhouse gases are relevant for predictions of climate warming, especially in a rapidly warming Arctic with huge C stocks in permafrost soils (McGuire et al., 2018). More variability alone resulted in a large, significant loss of C from the ecosystem (536 g C m^{-2}, Figure 5; Table 2). This loss is striking considering that the Arctic is currently

near C balance with respect to the atmosphere (McGuire et al., 2018). Even when combined with an imposed climate trend, more weather variability always reduced the C stored in vegetation, soil, and the whole ecosystem (total-ecosystem reduction of 206 g C m^{-2} below the control, Figure 5); a similar masking of the response to climate forcing has been found for internally generated variability arising from uncertainty in initial conditions for other models (Bonan et al., 2021). However, given the uncertainty on the sign of current or future changes in weather variability, the critical result here is that *either* more or less day-to-day weather variability could act as a powerful lever on the balance of C storage on land or loss to the atmosphere. In addition, the same mechanistic processes that regulate nutrient cycling and C storage in our biogeochemical model operate in all ecosystems, and we suggest that there should be analogous effects of day-to-day weather variability in most if not all biomes, although the sensitivity to individual weather variables will differ with the nature of limitation (e.g., temperature in arctic tundra vs. precipitation in mesic grasslands; Knapp et al., 2002). A final implication of our analyses is that changes in day-to-day weather variability are apparent within years to decades (Figure 2) and might therefore manifest sooner than the full effect of responses to predicted long-term mean trends in climate.

Although it is still unclear if weather variability is increasing (Alexander et al., 2006; Bathiany et al., 2018; Donat & Alexander, 2012) or decreasing (Blackport et al., 2021; Dai & Deng, 2021), it might be possible to detect at least initial effects of changes in weather variability for specific sites (e.g., rainfall manipulation, using eddy covariance data). However, only the initial effects of Jensen's inequality are likely to be detected in comparisons of years with low variability to years with high variability. Longer, persistent changes in day-to-day weather variability will be required for the ecosystem-level feedbacks that underly the most important results of our analysis to become manifest. Our analysis is based on the resource-optimization perspective embodied in the MEL model (Rastetter, Kwiatkowski, et al., 2022). A comparison of the results of similar analyses among different models could identify key hypotheses, long-term monitoring strategies, or the best empirical approach to test the effects of changes in day-to-day variability on ecosystem C storage (Rastetter, 1996).

Our predicted response of arctic tundra to climate trends is within the wide range of responses predicted by other models for tundra and boreal ecosystems (McGuire et al., 2018). To this large uncertainty among models our results add the uncertainty of how weather variability will change as climate changes and the uncertainty associated with how ecosystems will respond to that change in weather variability. Thus, our most important conclusion is not in the magnitude of the response predicted by our model, but rather in the recognition that changes in weather variability can have significant effects on C sequestration in ecosystems and the exchange of C between ecosystems and the atmosphere.

AUTHOR CONTRIBUTIONS

George W. Kling, Edward B. Rastetter, Kevin L. Griffin, and Bonnie L. Kwiatkowski contributed to the conceptualization and interpretation of the study and to the writing, review and editing of the manuscript. Edward B. Rastetter and Bonnie L. Kwiatkowski developed the methodology. Edward B. Rastetter, Kevin L. Griffin, and George W. Kling acquired funding for the study.

ACKNOWLEDGMENTS

This research was supported by the National Science Foundation grants DEB-1637459 (E.B.R., G.W.K.), DEB-2220863 (K.L.G., G.W.K.), DEB-2224743 (K.L.G., E.B.R., G.W.K.) DEB-1753731 (G.W.K.), OPP-1936769 (G.W.K.), DEB-1651722 (E.B.R.), and DEB-1556772 (E.B.R.). We also thank R. Cory and D. Menge for constructive criticism on the manuscript.

CONFLICT OF INTEREST STATEMENT

The authors declare that they have no conflicts of interest.

DATA AVAILABILITY STATEMENT

The data that support the finding of this study are openly available on the Environmental Data Initiative Data Portal at https://doi.org/10.6073/pasta/a946904960bb11f44915b80fb4fc5981 and https://doi.org/10.6073/pasta/83775003d8ef8978bf43d5c801f2a9a9. These data were derived from the following resources available in the public domain: https://doi.org/10.6073/pasta/c37707dcee5c9bc55b3fc7599e784010 and https://doi.org/10.6073/pasta/1735708437b5f6f755c3fc34910213a0. Source code and full model equations for MEL v2.8.5, are available on Zenodo (https://zenodo.org/record/6502583#YmrnBNPMKUk) and GitHub (https://github.com/bkwiatkowski/MELVI).

ORCID

Edward B. Rastetter https://orcid.org/0000-0002-8620-5431
Kevin L. Griffin https://orcid.org/0000-0003-4124-3757
Bonnie L. Kwiatkowski https://orcid.org/0000-0003-0158-9753
George W. Kling https://orcid.org/0000-0002-6349-8227

REFERENCES

Alexander, L. V., Zhang, X., Peterson, T. C., Caesar, J., Gleason, B., Klein Tank, A. M. G., Haylock, M., Collins, D., Trewin, B., Rahimzadeh, F., & Tagipour, A. (2006). Global observed changes in daily climate extremes of temperature and precipitation. *Journal of Geophysical Research: Atmospheres*, *111*(D5), 290. https://doi.org/10.1029/2005JD006290

Arora, V. K., Katavouta, A., Williams, R. G., Jones, C. D., Brovkin, V., Friedlingstein, P., Schwinger, J., Bopp, L., Boucher, O., Cadule, P., & Chamberlain, M. A. (2020). Carbon–concentration and carbon–climate feedbacks in CMIP6 models and their comparison to CMIP5 models. *Biogeosciences*, *17*(16), 4173–4222. https://doi.org/10.5194/bg-17-4173-2020

Baldocchi, D., Chu, H., & Reichstein, M. (2018). Inter-annual variability of net and gross ecosystem carbon fluxes: A review. *Agricultural and Forest Meteorology*, *249*, 520–533. https://doi.org/10.1016/j.agrformet.2017.05.015

Bathiany, S., Dakos, V., Scheffer, M., & Lenton, T. M. (2018). Climate models predict increasing temperature variability in poor countries. *Science Advances*, *4*(5), eaar5809. https://doi.org/10.1126/sciadv.aar5809

Bernhardt, J. R., O'Connor, M. I., Sunday, J. M., & Gonzalez, A. (2020). Life in fluctuating environments. *Philosophical Transactions of the*

Royal Society B, *375*(1814), 20190454. https://doi.org/10.1098/rstb.2019.0454

Blackport, R., Fyfe, J. C., & Screen, J. A. (2021). Decreasing subseasonal temperature variability in the northern extratropics attributed to human influence. *Nature Geoscience*, *14*(10), 719–723. https://doi.org/10.1038/s41561-021-00826-w

Bonan, G. B., Lombardozzi, D. L., & Wieder, W. R. (2021). The signature of internal variability in the terrestrial carbon cycle. *Environmental Research Letters*, *16*(3), 034022. https://doi.org/10.1088/1748-9326/abd6a9

Campbell, J. L., Rustad, L. E., Boyer, E. W., Christopher, S. F., Driscoll, C. T., Fernandez, I. J., Groffman, P. M., Houle, D., Kiekbusch, J., Magill, A. H., & Mitchell, M. J. (2009). Consequences of climate change for biogeochemical cycling in forests of northeastern North America. *Canadian Journal of Forest Research*, *39*(2), 264–284. https://doi.org/10.1139/X08-104

Cleverly, J., Eamus, D., Edwards, W., Grant, M., Grundy, M. J., Held, A., Karan, M., Lowe, A. J., Prober, S. M., Sparrow, B., & Morris, B. (2019). TERN, Australia's land observatory: Addressing the global challenge of forecasting ecosystem responses to climate variability and change. *Environmental Research Letters*, *14*(9), 095004. https://doi.org/10.1088/1748-9326/ab33cb

Dai, A., & Deng, J. (2021). Arctic amplification weakens the variability of daily temperatures over northern middle-high latitudes. *Journal of Climate*, *34*(7), 2591–2609. https://doi.org/10.1175/JCLI-D-20-0514.1

De Boeck, H. J., Bloor, J. M., Kreyling, J., Ransijn, J. C., Nijs, I., Jentsch, A., & Zeiter, M. (2018). Patterns and drivers of biodiversity–stability relationships under climate extremes. *Journal of Ecology*, *106*(3), 890–902. https://doi.org/10.1111/1365-2745.12897

Donat, M. G., & Alexander, L. V. (2012). The shifting probability distribution of global daytime and night-time temperatures. *Geophysical Research Letters*, *39*(14), 459. https://doi.org/10.1029/2012GL052459

Eby, M., Weaver, A. J., Alexander, K., Zickfeld, K., Abe-Ouchi, A., Cimatoribus, A. A., Crespin, E., Drijfhout, S. S., Edwards, N. R., Eliseev, A. V., & Feulner, G. (2013). Historical and idealized climate model experiments: An intercomparison of Earth system models of intermediate complexity. *Climate of the Past*, *9*, 1111–1140. https://doi.org/10.5194/cp-9-1111-2013

Environmental Data Center Team. (2021). *Meteorological monitoring program at Toolik, Alaska*. Toolik Field Station, Institute of Arctic Biology, University of Alaska Fairbanks. http://toolik.alaska.edu/edc/abiotic_monitoring/data_query.php

Estiarte, M., Vicca, S., Peñuelas, J., Bahn, M., Beier, C., Emmett, B. A., Fay, P. A., Hanson, P. J., Hasibeder, R., Kigel, J., & Kröel-Dulay, G. (2016). Few multiyear precipitation–reduction experiments find a shift in the productivity–precipitation relationship. *Global Change Biology*, *22*(7), 2570–2581. https://doi.org/10.1111/gcb.13269

Gherardi, L. A., & Sala, O. E. (2019). Effect of interannual precipitation variability on dryland productivity: A global synthesis. *Global Change Biology*, *25*(1), 269–276. https://doi.org/10.1111/gcb.14480

Hou, E., Litvak, M. E., Rudgers, J. A., Jiang, L., Collins, S. L., Pockman, W. T., Hui, D., Niu, S., & Luo, Y. (2021). Divergent responses of primary production to increasing precipitation variability in global drylands. *Global Change Biology*, *27*(20), 5225–5237. https://doi.org/10.1111/gcb.15801

Hughes, T. P., Kerry, J. T., Connolly, S. R., Baird, A. H., Eakin, C. M., Heron, S. F., Hoey, A. S., Hoogenboom, M. O., Jacobson, M., Liu, G., Pratchett, M. S., Skirving, W., & Torda, G. (2019). Ecological memory modifies the cumulative impact of recurrent climate extremes. *Nature Climate Change*, *9*(1), 40–43. https://doi.org/10.1038/s41558-018-0351-2

Huxman, T. E., Smith, M. D., Fay, P. A., Knapp, A. K., Shaw, M. R., Loik, M. E., Smith, S. D., Tissue, D. T., Zak, J. C., Weltzin, J. F., Pockman, W. T., Sala, O. E., Haddad, B. M., Harte, J., Koch, G. W., Schwinning, S., Small, E. E., & Williams, D. G. (2004). Convergence across biomes to a common rain-use efficiency. *Nature*, *429*(6992), 651–654. https://doi.org/10.1038/nature02561

Iverson, L. R., Thompson, F. R., Matthews, S., Peters, M., Prasad, A., Dijak, W. D., Fraser, J., Wang, W. J., Hanberry, B., He, H., Janowiak, M., Butler, P., Brandt, L., & Swanston, C. (2017). Multi-model comparison on the effects of climate change on tree species in the eastern US: Results from an enhanced niche model and process-based ecosystem and landscape models. *Landscape Ecology*, *32*, 1327–1346. https://doi.org/10.1007/s10980-016-0404-8

Jensen, J. L. W. V. (1906). Sur les fonctions convexes et les inégalités entre les valeurs moyennes. *Acta Mathematica*, *30*(1), 175–193. https://doi.org/10.1007/BF02418571

Jiang, Y., Rastetter, E. B., Rocha, A. V., Pearce, A. R., Kwiatkowski, B. L., & Shaver, G. R. (2015). Modeling carbon–nutrient interactions during the early recovery of tundra after fire. *Ecological Applications*, *25*(6), 1640–1652. https://doi.org/10.1890/14-1921.1

Keenan, T., Sabate, S., & Gracia, C. (2010). Soil water stress and coupled photosynthesis–conductance models: Bridging the gap between conflicting reports on the relative roles of stomatal, mesophyll conductance and biochemical limitations to photosynthesis. *Agricultural and Forest Meteorology*, *150*(3), 443–453. https://doi.org/10.1016/j.agrformet.2010.01.008

Kim, J., & Verma, S. B. (1991). Modeling canopy stomatal conductance in a temperate grassland ecosystem. *Agricultural and Forest Meteorology*, *55*(1–2), 149–166. https://doi.org/10.1016/0168-1923(91)90028-O

Knapp, A. K., Beier, C., Briske, D. D., Classen, A. T., Luo, Y., Reichstein, M., Smith, M. D., Smith, S. D., Bell, J. E., Fay, P. A., Heisler, J. L., Leavitt, S. W., Sherry, R., Smith, B., & Weng, E. (2008). Consequences of more extreme precipitation regimes for terrestrial ecosystems. *Bioscience*, *58*(9), 811–821. https://doi.org/10.1641/B580908

Knapp, A. K., Fay, P. A., Blair, J. M., Collins, S. L., Smith, M. D., Carlisle, J. D., Harper, C. W., Danner, B. T., Lett, M. S., & McCarron, J. K. (2002). Rainfall variability, carbon cycling, and plant species diversity in a mesic grassland. *Science*, *298*(5601), 2202–2205. https://doi.org/10.1126/science.1076347

Knapp, A. K., & Smith, M. D. (2001). Variation among biomes in temporal dynamics of aboveground primary production. *Science*, *291*(5503), 481–484. https://doi.org/10.1126/science.291.5503.481

Lauenroth, W. K., & Sala, O. E. (1992). Long-term forage production of North American shortgrass steppe. *Ecological Applications*, *2*(4), 397–403. https://doi.org/10.2307/1941874

Luo, Y., Gerten, D., Le Maire, G., Le Maire, G., Parton, W. J., Weng, E., Zhou, X., Keough, C., Beier, C., Ciais, P., Cramer, W., Dukes, J. S., Emmett, B., Hanson, P. J., Knapp, A., Linder, S., Nepstad, D., & Rustad, L. (2008). Modeled interactive effects of precipitation, temperature, and [CO_2] on ecosystem carbon and water dynamics in different climatic zones. *Global Change Biology*, *14*, 1986–1999. https://doi.org/10.1111/j.1365-2486.2008.01629.x

Luo, Y., & Weng, E. (2011). Dynamic disequilibrium of the terrestrial carbon cycle under global change. *Trends in Ecology & Evolution*, *26*(2), 96–104. https://doi.org/10.1016/j.tree.2010.11.003

McGuire, A. D., Lawrence, D. M., Koven, C., Clein, J. S., Burke, E., Chen, G., Jafarov, E., MacDougall, A. H., Marchenko, S., Nicolsky, D., Peng, S., Rinke, A., Ciais, P., Gouttevin, I., Hayes, D. J., Ji, D., Krinner, G., Moore, J. C., Romanovsky, V., … Zhuang, Q. (2018). Dependence of the evolution of carbon dynamics in the northern permafrost region on the trajectory of climate change. *Proceedings of the National Academy of Sciences of the United States of America*, *115*(15), 3882–3887. https://doi.org/10.1073/pnas.1719903115

Medvigy, D., Wofsy, S. C., Munger, J. W., & Moorcroft, P. R. (2010). Responses of terrestrial ecosystems and carbon budgets to current and future environmental variability. *Proceedings of the National Academy of Sciences of the United States of America*, *107*(18), 8275–8280. https://doi.org/10.1073/pnas.0912032107

Monier, E., Kicklighter, D. W., Sokolov, A. P., Zhuang, Q., Sokolik, I. N., Lawford, R., Kappas, M., Paltsev, S. V., & Groisman, P. Y. (2017). A

review of and perspectives on global change modeling for Northern Eurasia. *Environmental Research Letters*, *12*(8), 083001. https://doi.org/10.1088/1748-9326/aa7aae

Monier, E., Paltsev, S., Sokolov, A., Chen, Y. H. H., Gao, X., Ejaz, Q., Couzo, E., Schlosser, C. A., Dutkiewicz, S., Fant, C., Scott, J., Kicklighter, D., Morris, J., Jacoby, H., Prinn, R., & Haigh, M. (2018). Toward a consistent modeling framework to assess multi-sectoral climate impacts. *Nature Communications*, *9*(1), 660. https://doi.org/10.1038/s41467-018-02984-9

Paschalis, A., Fatichi, S., Katul, G. G., & Ivanov, V. Y. (2015). Cross-scale impact of climate temporal variability on ecosystem water and carbon fluxes. *Journal of Geophysical Research: Biogeosciences*, *120*(9), 1716–1740. https://doi.org/10.1002/2015JG003002

Pearce, A. R., Rastetter, E. B., Kwiatkowski, B. L., Bowden, W. B., Mack, M. C., & Jiang, Y. (2015). Recovery of arctic tundra from thermal erosion disturbance is constrained by nutrient accumulation: A modeling analysis. *Ecological Applications*, *25*(5), 1271–1289. https://doi.org/10.1890/14-1323.1

Rammig, A., & Mahecha, M. D. (2015). Ecosystem responses to climate extremes. *Nature*, *527*(7578), 315–316. https://doi.org/10.1038/527315a

Rastetter, E., Griffin, K., Kwiatkowski, B., & Kling, G. (2022a). *Weather measurements for Toolik Lake, Alaska, 1989–2019 ver 1*. Environmental Data Initiative. https://doi.org/10.6073/pasta/c37707dcee5c9bc55b3fc7599e784010

Rastetter, E., Griffin, K., Kwiatkowski, B., & Kling, G. (2022b). *Model simulations of the effects of shifts in high-frequency weather variability (no long-term trend) on carbon loss from land to the atmosphere, Toolik Lake, Alaska, 2022–2122 ver 3*. Environmental Data Initiative. https://doi.org/10.6073/pasta/a946904960bb11f44915b80fb4fc5981

Rastetter, E., Griffin, K., Kwiatkowski, B., & Kling, G. (2022c). *Model simulations of the effects of shifts in high-frequency weather variability (with a long-term trend) on carbon loss from land to the atmosphere, Toolik Lake, Alaska, 2022–2122 ver 3*. Environmental Data Initiative. https://doi.org/10.6073/pasta/83775003d8ef8978bf43d5c801f2a9a9

Rastetter, E. B. (1996). Validating models of ecosystem response to global change. *Bioscience*, *46*(3), 190–198. https://doi.org/10.2307/1312740

Rastetter, E. B., Ågren, G. I., & Shaver, G. R. (1997). Responses of N-limited ecosystems to increased CO_2: A balanced-nutrition, coupled-element-cycles model. *Ecological Applications*, *7*(2), 444–460. https://doi.org/10.1890/1051-0761(1997)007[0444:RONLET]2.0.CO;2

Rastetter, E. B., King, A. W., Cosby, B. J., Hornberger, G. M., O'Neill, R. V., & Hobbie, J. E. (1992). Aggregating fine-scale ecological knowledge to model coarser-scale attributes of ecosystems. *Ecological Applications*, *2*(1), 55–70. https://doi.org/10.2307/1941889

Rastetter, E. B., & Kwiatkowski, B. L. (2020). An approach to modeling resource optimization for substitutable and interdependent resources. *Ecological Modelling*, *425*, 109033. https://doi.org/10.1016/j.ecolmodel.2020.109033

Rastetter, E. B., Kwiatkowski, B. L., Kicklighter, D. W., Barker Plotkin, A., Genet, H., Nippert, J. B., O'Keefe, K., Perakis, S. S., Porder, S., Roley, S. S., Ruess, R. W., Thompson, J., Weider, W. R., Wilcox, K., & Yanai, R. D. (2022). N and P constrain C in ecosystems under climate change: Role of nutrient redistribution, accumulation, and stoichiometry. *Ecological Applications*, *32*(8), e2684. https://doi.org/10.1002/eap.2684

Rastetter, E. B., & Shaver, G. R. (1992). A model of multiple-element limitation for acclimating vegetation. *Ecology*, *73*(4), 1157–1174. https://doi.org/10.2307/1940666

Rastetter, E. B., Yanai, R. D., Thomas, R. Q., Vadeboncoeur, M. A., Fahey, T. J., Fisk, M. C., Kwiatkowski, B. L., & Hamburg, S. P. (2013). Recovery from disturbance requires resynchronization of ecosystem nutrient cycles. *Ecological Applications*, *23*(3), 621–642. https://doi.org/10.1890/12-0751.1

Rollinson, C. R., Liu, Y., Raiho, A., Moore, D. J., McLachlan, J., Bishop, D. A., Dye, A., Matthes, J. H., Hessl, A., Hickler, T., Pederson, N., Poulter, B., Quaife, T., Schaefer, K., Steinkamp, J., & Dietze, M. C. (2017). Emergent climate and CO_2 sensitivities of net primary productivity in ecosystem models do not agree with empirical data in temperate forests of eastern North America. *Global Change Biology*, *23*(7), 2755–2767. https://doi.org/10.1111/gcb.13626

Rudgers, J. A., Chung, Y. A., Maurer, G. E., Moore, D. I., Muldavin, E. H., Litvak, M. E., & Collins, S. L. (2018). Climate sensitivity functions and net primary production: A framework for incorporating climate mean and variability. *Ecology*, *99*(3), 576–582. https://doi.org/10.1002/ecy.2136

Ruel, J. J., & Ayres, M. P. (1999). Jensen's inequality predicts effects of environmental variation. *Trends in Ecology & Evolution*, *14*(9), 361–366. https://doi.org/10.1016/S0169-5347(99)01664-X

Sala, O. E., Parton, W. J., Joyce, L. A., & Lauenroth, W. K. (1988). Primary production of the central grassland region of the United States. *Ecology*, *69*(1), 40–45. https://doi.org/10.2307/1943158

Seddon, A. W., Macias-Fauria, M., Long, P. R., Benz, D., & Willis, K. J. (2016). Sensitivity of global terrestrial ecosystems to climate variability. *Nature*, *531*(7593), 229–232. https://doi.org/10.1038/nature16986

Shaver, G. R., Laundre, J. A., Bret-Harte, M. S., Chapin, F. S., Mercado-Díaz, J. A., Giblin, A. E., Gough, L., Gould, W. A., Hobbie, S. E., Kling, G. W., Mack, M. C., Moore, J. C., Nadelhoffer, K. J., Rastetter, E. B., & Schimel, J. P. (2014). Terrestrial ecosystems at Toolik lake, Alaska. In J. Hobbie & G. W. Kling (Eds.), *Alaska's changing Arctic: Ecological consequences for tundra, streams and lakes* (pp. 90–142). Oxford University Press. https://doi.org/10.1093/acprof:osobl/9780199860401.003.0005

Snedecor, G. W., & Cochran, W. G. (1967). *Statistical methods* (6th ed.). Iowa State University Press.

Templeton, A. R., & Lawlor, L. R. (1981). The fallacy of the averages in ecological optimization theory. *The American Naturalist*, *117*(3), 390–393. https://doi.org/10.1086/283719

Valipour, M., Johnson, C. E., Battles, J. J., Campbell, J. L., Fahey, T. J., Fakhraei, H., & Driscoll, C. T. (2021). Simulation of the effects of forest harvesting under changing climate to inform long-term sustainable forest management using a biogeochemical model. *Science of the Total Environment*, *767*, 144881. https://doi.org/10.1016/j.scitotenv.2020.144881

Wang, W. J., Ma, S., He, H. S., Liu, Z., Thompson, F. R., Jin, W., Wu, Z. F., Spetich, M. A., Wang, L., Xue, S., Zhang, W., & Wang, X. (2019). Effects of rising atmospheric CO_2, climate change, and nitrogen deposition on aboveground net primary production in a temperate forest. *Environmental Research Letters*, *14*(10), 104005. https://doi.org/10.1088/1748-9326/ab3178

Wu, C., Chen, Y., Peng, C., Li, Z., & Hong, X. (2019). Modeling and estimating aboveground biomass of *Dacrydium pierrei* in China using machine learning with climate change. *Journal of Environmental Management*, *234*, 167–179. https://doi.org/10.1016/j.jenvman.2018.12.090

SUPPORTING INFORMATION

Additional supporting information can be found online in the Supporting Information section at the end of this article.

How to cite this article: Rastetter, E. B., Griffin, K. L., Kwiatkowski, B. L., & Kling, G. W. (2023). Ecosystem feedbacks constrain the effect of day-to-day weather variability on land–atmosphere carbon exchange. *Global Change Biology*, *29*, 6093–6105. https://doi.org/10.1111/gcb.16926